

## Post Thermal Oxidation of Tin Thin Film on Silicon Substrate for MIS Hetrojunction Prepared by Thermal Evaporation

Halah H. Rashed

Applied Science Department, University of Technology/Baghdad.

Email:hala\_hassan8140@yahoo.com

Received on:29/6/2015 & Accepted on:20/1/2016

### ABSTRACT

In this work, preparation of high quality conductive oxide SnO<sub>2</sub> thin film by post-thermal treatment of deposited tin by vacuum thermal evaporation on glass and p -type silicon substrates for preparation of metal-insulator-semiconductor hetrojunction.

The optical absorption, electrical, structural and surface morphology of the SnO<sub>2</sub> thin film on glass substrate were characterized by UV-VIS-NIR spectrophotometer, electrical conductivity, X-ray diffraction spectrum and atomic force microscope respectively.

The X-Ray Diffraction pattern show that the SnO<sub>2</sub> thin film is polycrystalline with tetragonal rutile, Atomic Force Microscope show that the grains size of the thin film varies from 50 to 150 nm .The optical properties show that SnO<sub>2</sub> thin film is high absorbance in Ultra-violet region, whereas it's transparent in the visible and near infrared regions and have direct optical band gap of 3.6 eV, and last the electrical conductivity results show that the resistivity is decrease with increase the temperature and activation energy is approximately to the 0.107eV.

The electrical properties of n SnO<sub>2</sub>/SiO<sub>2</sub>/p Si hetrojunction were studied by I-V measurement under dark and illumination conditions, in the dark condition, I-V measurement reveals that the hetrojunction have rectifying behavior, the ideality factor and the reverse saturation current of this diode are 5.18 and  $1.5 \times 10^{-6}$  A respectively. Under illumination condition, I-V measurement reveals that the photocurrent is larger than the dark current, and a linear relation between I<sub>SC</sub> and V<sub>OC</sub> with the incident light intensity to reach a maximum value beyond tends to saturated and become constant. These electrical properties of prepared device can its work as a detector or solar cell.

**Keywords:** SnO<sub>2</sub> Thin Film, Vacuum Thermal Evaporation, MIS hetrojunction

### INTRODUCTION

There has been considerable interest in recent years directed toward the development of metal-insulator-semiconductor (MIS) solar cells. Very often in these structures, tin dioxide (SnO<sub>2</sub>), indium tin oxide (ITO), and zinc oxide (ZnO) were used in place of the metal electrode [1]. The top semiconductor film with wide band gap can serve as an antireflection coating [2], a low-resistance window, as the collector of the p-n junction and can eliminate the surface dead layer which often occurs within the homojunction devices. On the other side, this absence of the light absorption of visible region in a surface layer can improve the ultraviolet response of the internal quantum efficiency [3]. Among many transparent conductive oxides (TCO) of transition metals, Tin dioxide (SnO<sub>2</sub>) is chosen because it's have many advantages such as an important n-type semiconductor with a wide-direct band gap of (E<sub>g</sub>=3.6 ~ 4.2 eV)[4], highly absorption coefficient in the UV region, whereas it's transparent in the visible and infrared regions [5], it is very stable, has got high carrier density and supports

enormous concentration of intrinsic and stoichiometry-violating vacancies, which is correlated to its electrical conductivity [6].

These advantages of SnO<sub>2</sub> make it very suitable in many applications such as solar cells [7], Hydrogen Sensing [8], Resistive switching random access memory [9], Electronic Devices and Micro Electromechanical Systems (MEMS) [10] and MIS device [11]

Hence, considerable efforts have been made to fabricate SnO<sub>2</sub> nanostructures via various methods, such as chemical spray pyrolysis [4], sol-gel [12] Solvothermal Synthesis Method [13] electron beam evaporated [14] pulsed laser deposition and pulsed laser ablation in liquid [15] Among these methods, vacuum thermal evaporation [2,16] has advantages due to its simplicity and high-quality products.

The electrical properties of the SnO<sub>2</sub> thin film can give a clear idea regarding the transport mechanism related to electrical conduction which gives the value of electrical resistivity ( $\rho$ ) and conductivity ( $\sigma$ ) of film. There are various models to explain the conduction process in poly crystalline film based on different scattering mechanisms.

The film resistivity, however, may be due to a combination of three mechanisms, namely (1) Due to scattering from phonon, impurities and point defects, etc. (2) From film surface, (3) Due to grain boundaries which would be predominant in poly crystalline film [17].

### Experimental work

Metallic tin powder 99.99% pure and 0.137 gram in weight is measured from weighing method using digital weight balance (to obtain the desired thickness of the thin film) was placed in a molybdenum boat as vapor source and deposited on glass substrate with dimensions (2×2.6×0.1 cm<sup>3</sup>) and on p-type silicon of (1.5–4) Ω·cm with dimensions (0.5×0.6 cm<sup>2</sup>) by vacuum thermal evaporation technique. Glass slide cleaned with ethanol and distilled water and silicon substrate is cleaned with HF and distilled water to remove impurities. The evaporation was carried out on the substrates at room temperature in a vacuum of about (7×10<sup>-5</sup>) torr, The substrate was located at a distance of 15 cm from the evaporated source. The base pressure was achieved by diffusion pump which produces very low pressure down to (10<sup>-3</sup>-10<sup>-6</sup>) torr backed by a mechanical pump (rotary pump) which is called roughing stage where the vacuum can reach 10<sup>-2</sup> torr. Figure (1) show the thermal evaporator compound used in this work.

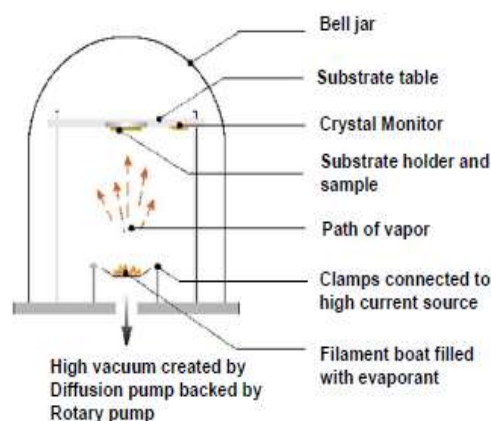


Figure.(1) thermal evaporator compounds

After deposition of Sn thin films on glass and silicon substrate, put the films in oven at atmosphere pressure at 600C° temperature and 2 hour oxidation time to prepare SnO<sub>2</sub> thin film

on glass substrate and SnO<sub>2</sub>/SiO<sub>2</sub>/Si hetrojunction respectively. Figure (2) show the calibration curve of the thermal oxidation where two distinct regions are noticed. In the first region, the temperature increase with increasing the time, while in the second region the temperature was constant with the increasing the time and it is in this region where thermal oxidation was accomplished.

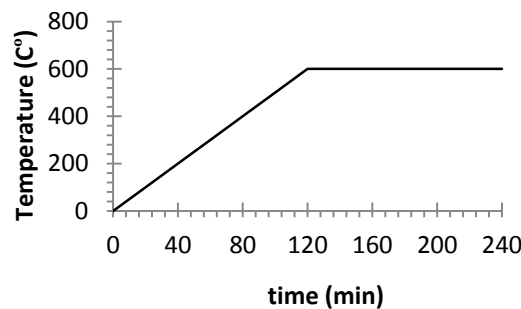


Figure. (2) Scheme for the calibration system of thermal oxidation.

Two methods were used to measure the thickness of thin film, the weight method and optical interferometric method. In the first method the theoretical formula is used given by: [18]

$$t = \frac{m}{2\pi \rho R} \dots \dots \dots (1)$$

Where: m is the mass of the material, ρ is the density of the material, R is the distance between the substrate and the boat.

In the second method employing He-Ne laser (632.8 nm) with incident angle 45° as shown schematically in figure (3).

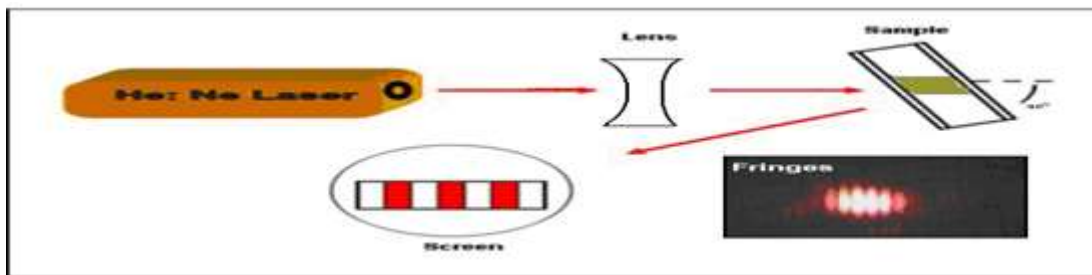


Figure. (3)The schematic diagram of the film thickness measurement.

This method depends on the interference of the laser beam reflected from thin film surface and substrate, film thickness (t) was determined using the following formula:

$$t = \frac{\Delta x}{x} \cdot \frac{\lambda}{2} \dots \dots \dots (2)$$

Where (x) is the fringe width, (Δx) is the distance between two fringes and (λ) is the wavelength of He:Ne laser beam.

The optical properties of tin oxide thin film are measuring by using a double beam Shimadzu spectrophotometer with respect to a piece of glass similar to the substrates in the wavelength range from 300nm to 1100 nm. The crystal structure of tin oxide thin film on glass substrate characterized by X-Ray diffraction pattern from the target of Cu with 1.5406Å wavelength, XRD patterns were recorded range from 20 to 70 deg (2θ) with a scanning step of 0.05(deg) and surface morphology is measuring by atomic force microscope, the thin film conductivity respectively.

After thermal oxidation of the tin thin film on the silicon substrate at 600 C° and 2 hour, Aluminum with purity (99.99%) thin film was deposited as back contact for the fabricated sample for Ohmic contact.

**Results and Discussions**

**- Characterization of tin oxide thin film deposited on the glass substrate**

The structure properties of tin oxide film on the glass substrate at 600 C° oxidation temperature and 2 hour oxidation time is studied by X-Ray diffraction pattern measurement as shown in

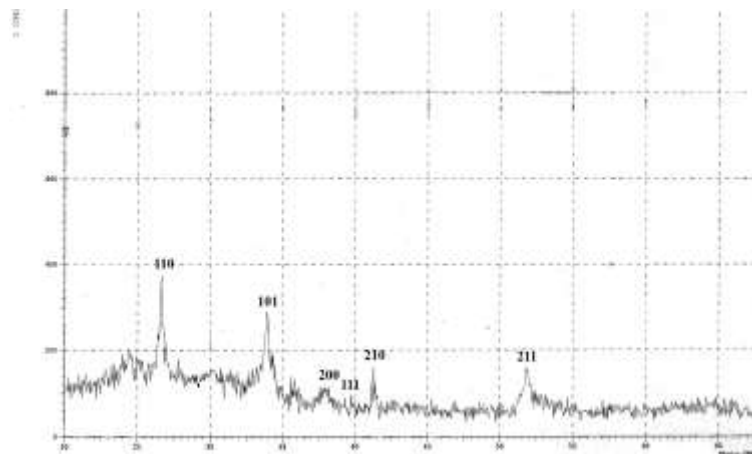


**Figure. (4):X-Ray diffraction pattern of Tin oxide thin film**

figure (4).

This figure show that the film is polycrystalline in structure, The diffraction peaks at 26.6°, 33.9°, 38.2°, 39.83°, 42.58° and 51.8° can be indexed to (110), (101), (200), (111), (210) and (211) lattice planes of the tetragonal rutile structure of SnO<sub>2</sub> confirmed by standard JCPDS data (card no.46-1088) [19], No peaks from impurities including Sn or SnO were detected.

The average grain size can be calculated by the using Scherrer formula: [20]

$$D g = \frac{K \lambda}{\beta \cos \theta} \dots \dots \dots (6)$$

Where D g is the average crystalline size, K is a constant (0.94) is the correction factor in the Debye Scherer equation, λ is the wavelength of incident X-ray radiation (1.5404 Å for CuKa), β is the FWHM of peaks and θ is the Bragg angle.

The structure parameters of tin oxide thin film are shown in table (1)

Diffraction angles(2θ) degree	I/I <sub>1</sub> XRD (intensity)	d (Å) XRD	(h k l) Miller indices	FWHM Degree	Grain size (nm)
26.6	100	3.34	110	0.412	3.39
33.9	93	2.63	101	0.448	0.40
38.2	12	2.34	200	0.28	0.58
39.8	12	2.26	111	0.2	1.43
42.5	25	2.21	210	0.30	5.45
51.8	25	1.76	211	0.35	11.39

Table (1) the hkl, FWHM and grain of SnO<sub>2</sub> thin film with tetragonal rutile structure obtained from XRD investigation

The surface morphology of the SnO<sub>2</sub> thin film is studied through atomic force microscope technique as shown in figure (5). Figure (5 a) shows that the morphology of the tin oxide thin film as grains are spherical in shapes and homogeneously distributed, which indicate the crystalline nature of the film. The average roughness and root mean square of the film are 8.27 nm and 10.5 nm respectively.

Figure (5 b) shows the percentage of SnO<sub>2</sub> thin film as a function of the grain size, this figure shows that the size of grains varies from 50 to 150 nm and the average diameter is 99 nm.

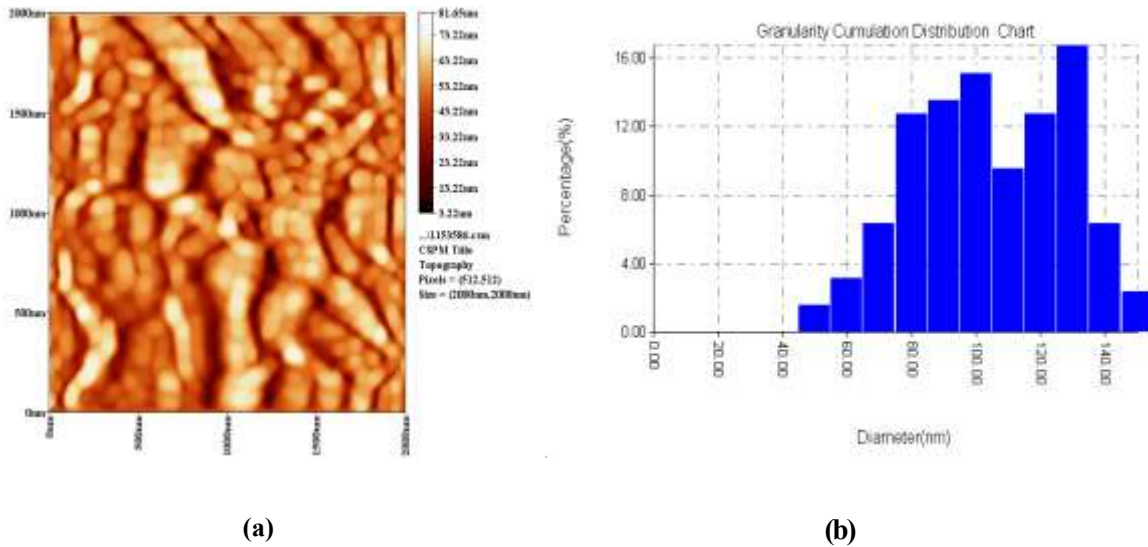
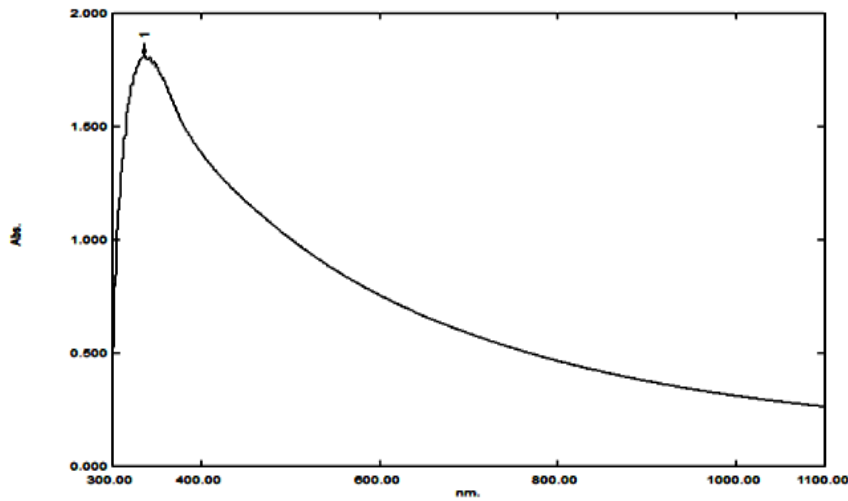


Figure. (5): a) atomic force microscope of SnO<sub>2</sub> thin film, b) Granularity Accumulation distribution Chart.

The optical absorption of SnO<sub>2</sub> thin film with 168 nm thickness is obtained by a UV-VIS-NIR Spectrophotometer in the wavelength range of 300nm to 1100nm and shown in the figure (6)



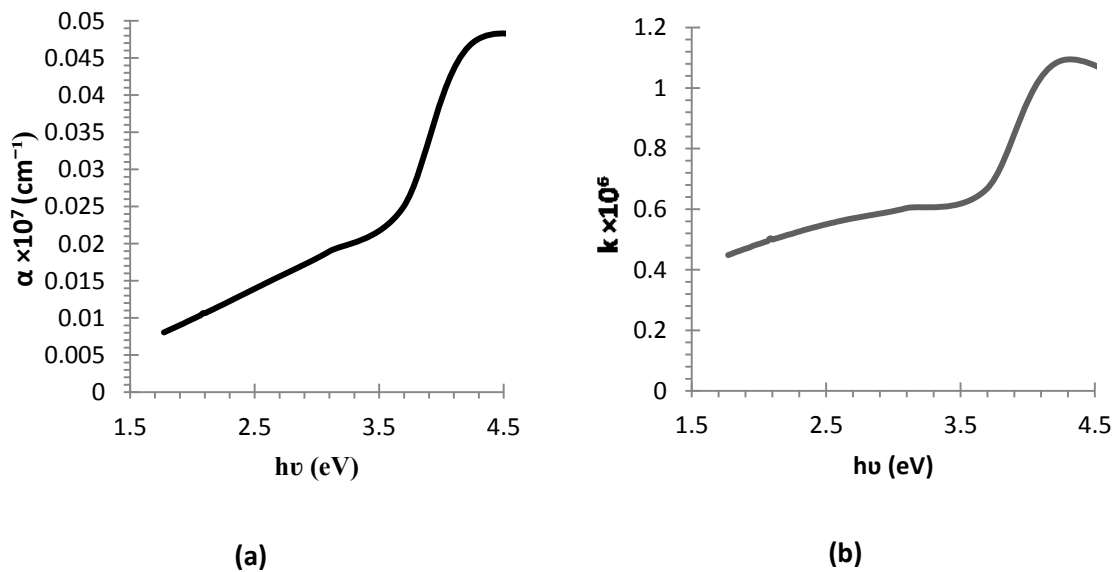
**Figure.(6): Optical absorption as a function of the wavelength for SnO<sub>2</sub> thin film prepared on glass substrate**

Figure (6) show the absorption peak of tin oxide thin film at 336 nm, and steep fall in the absorbance in the range from 400nm to the 1100 nm, this is meaning that the tin oxide is high absorbance in Ultra-violet region, whereas it's transparent in the visible and near infrared regions, Its caused by fundamental light absorption and by free-carrier absorption respectively. High optical absorbance of the thin film demonstrates the applicability of the film for photovoltaic applications. [21]

Absorption coefficient ( $\alpha$ ) associated with the strong absorption region of the sample was calculated from absorbent (A) and the sample thickness (t) was used the relation is related to Beer-Lambert law in 1852: [22]

$$\alpha = 2.303 \frac{A}{t} \dots \dots \dots (3)$$

Figure (7a) shows the absorption coefficient as function photon energy for SnO<sub>2</sub> thin film



**Figure.(7) a)Absorption coefficient as a function photon energy of SnO<sub>2</sub> thin film, b) Extinction coefficient as a function photon energy of SnO<sub>2</sub> thin film**

This figure shows the value of absorption coefficient is small in the low energy range then its value increase rapidly at the photon energy of 3.6 eV beyond absorption edge region.

Extinction coefficient (k) of tin oxide thin film was calculated by using the relation [22]:

$$k = \frac{\alpha \lambda}{4\pi} \dots \dots \dots (4)$$

Where  $\lambda$ : is the wavelength of the incident photon.

The extinction coefficient as a function of photon energy is shown in figure (6 b). This figure shows increase of the extinction coefficient with increase of the photon energy, this increase is directly related to the absorption of light. In the case of polycrystalline film, extra absorption of light occurs at the grain boundaries [23].This leads to non-zero value of k for photon energies smaller than the fundamental absorption edge.

The optical direct band gap energy ( $E_g$ ) of the tin oxide thin film is calculated from formula that many groups have used [24]

$$\alpha h\nu = A(h\nu - E_g)^{1/2} \dots \dots \dots (5)$$

The band gap can be deduced from a plot of  $(\alpha h\nu)^2$  versus photon energy (h $\nu$ ). The extrapolation of the linear portion of the  $(\alpha h\nu)^2$  vs. h $\nu$  plot to  $\alpha = 0$  will give the band gap value of the film [24].

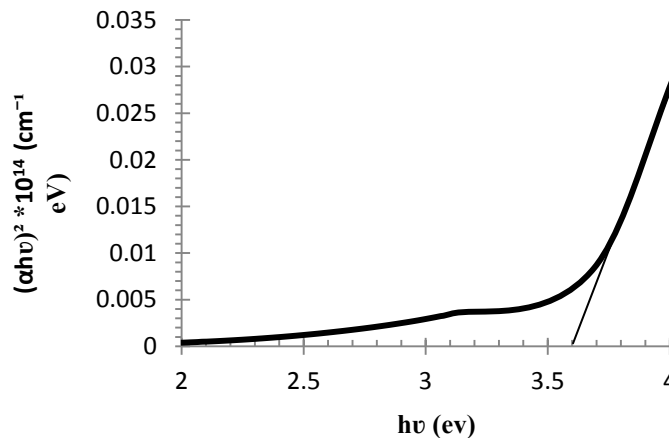


**Figure.(8): Plot of  $(\alpha h\nu)^2$  vs. photon energy(h $\nu$ ) of SnO<sub>2</sub> thin film with extrapolating straight line portion to evaluate the optical band gap of SnO<sub>2</sub>**

As presented in (Fig.8) the value of the optical band gap of SnO<sub>2</sub> thin film is 3.6eV for the almost in agreement with the reported values of band gap data by other workers .[5]

Figure (9 a, b) show the resistance is inversely proportional with the temperature while the logarithm of conductivity is increase with increasing the temperature for SnO<sub>2</sub> film. These variations in resistance and conductivity with temperature indicate the semiconducting behavior of the film suggesting a thermally activated conduction mechanism.

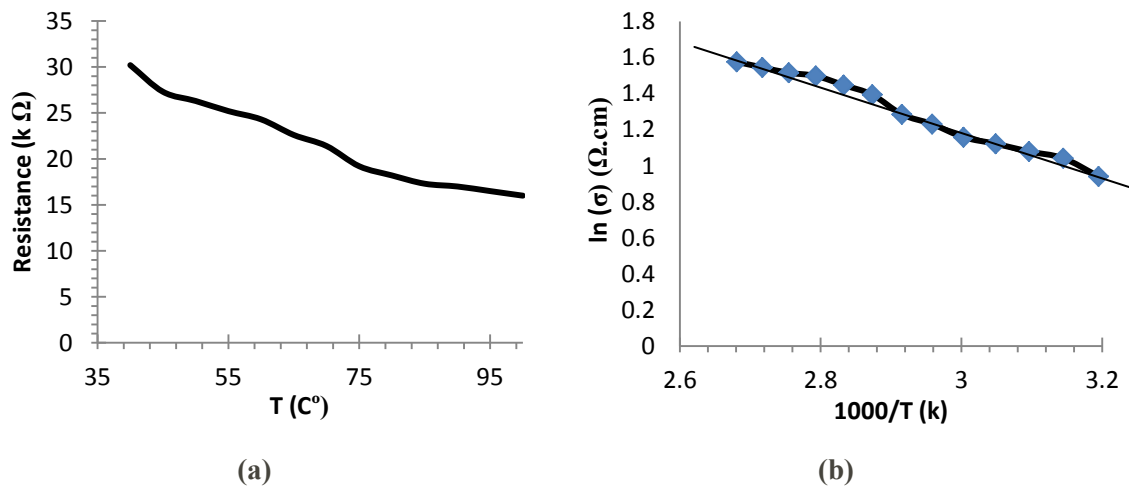


Figure.(9)(a,b) the Variation of resistance and electrical conductivity as a function of temperature T of SnO<sub>2</sub> thin film respectively

By calculating the slope in the Figure (9, b), can obtain the activation energy by using the equation [25]

$$\sigma = \sigma_0 \cdot \exp\left(\frac{-\Delta E_a}{KT}\right) \dots \dots \dots (6)$$

Where  $\sigma$  is the carrier conductivity,  $\Delta E_a$  is the activation energy,  $K$  is the Boltzmann constant and  $T$  is the temperature in absolute scale.

The activation energy has been determined by plotting graph between  $\ln(\sigma)$  versus  $1000/T$  as shown in figure (9.b) It is found that the activation energy for SnO<sub>2</sub> thin film is 0.107 eV.

It suggests that the conduction in the thin film is due to the thermally assisted tunneling of the charge carriers through the grain boundary

**- Characterization of MIS hetrojunction**

Figure (10) Shows the current–voltage characteristic of (n-SnO<sub>2</sub>/ SiO<sub>2</sub>/p-Si) at forward and reverse base in dark at room temperature.

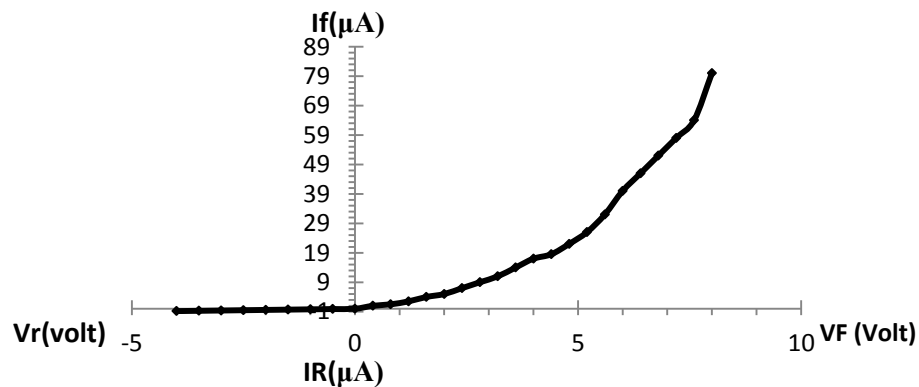


Figure.(10) current-voltage in forward and reverse bias of n SnO<sub>2</sub>-SiO<sub>2</sub>-p Si hetrojunction in the dark at room temperature

This figure show typical rectifying behavior, In the forward bias, Two regions are recognized; the first one represents recombination current, the first current established when the

concentration of the generated carrier is larger than the intrinsic carrier concentration ( $n_i$ ), i.e. ( $n \cdot p > n_i^2$ ), which lead to recombination process for mass low applicable. The second region at high voltage represented the diffusion or bending region which depending on serried resistance and in (MIS) case represented the tunneling region.

At 1 volt, the forward current increases exponentially because the bias voltage exceeds the potential barrier. This bias voltage gives the electrons energy to overcome the barrier height and flow that is called diffusion current.

In reverse bias, it is clear that the curve contains region represented the generation where the reverse current is slightly increased with the applied voltage and this tends to generation of electron-hole pairs at low bias.

While the dark current is a function of the applied bias, therefore the corresponding diode resistance defined as [11]

$$R_d = \left( \frac{dV}{dI} \right) \dots \dots \dots (7)$$

This equation is derived and shown in Figure (11).

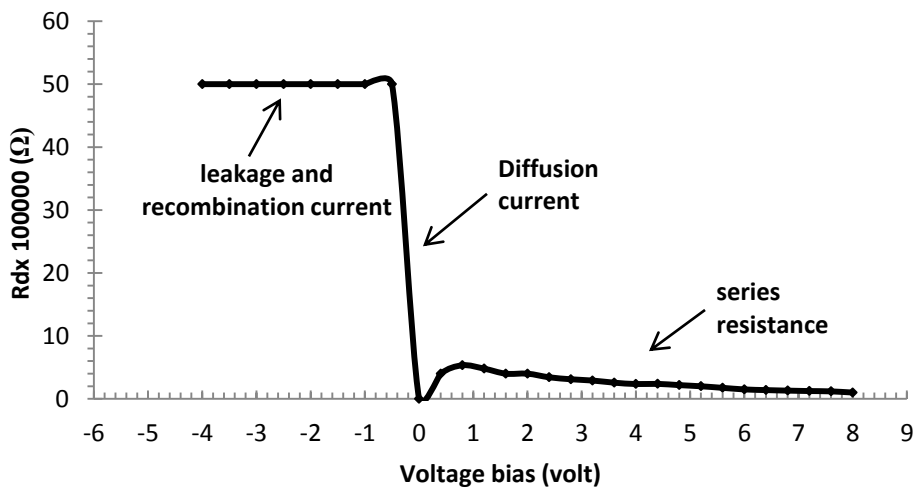


Figure. (11). The variation of diode resistance via Voltage bias in the dark current

The value of the ideality factor of the heterojunction is determined from the slop of the straight line region of the forward bias  $\log I-V$  characteristics as shown in the figure (12).

The turn-on voltage for the  $n\text{SnO}_2/\text{SiO}_2/p\text{-Si}$  heterojunction is about 1 V and the typical values of the ideality factor of this hetrojunction can calculated by using the equation [26]

$$n = \frac{q}{kT} \cdot \frac{\partial V}{\partial \ln I} \dots \dots \dots (8)$$

The ideality factor and reverse saturation current are 5.18 and  $1.5 \times 10^{-6}$  A respectively. The value of ideality factor is greater than unity which can be attributed to the recombination of electrons and holes in the depletion region as well as the tunneling effect depending on both sides of the heterojunction and on the presence of defect state.

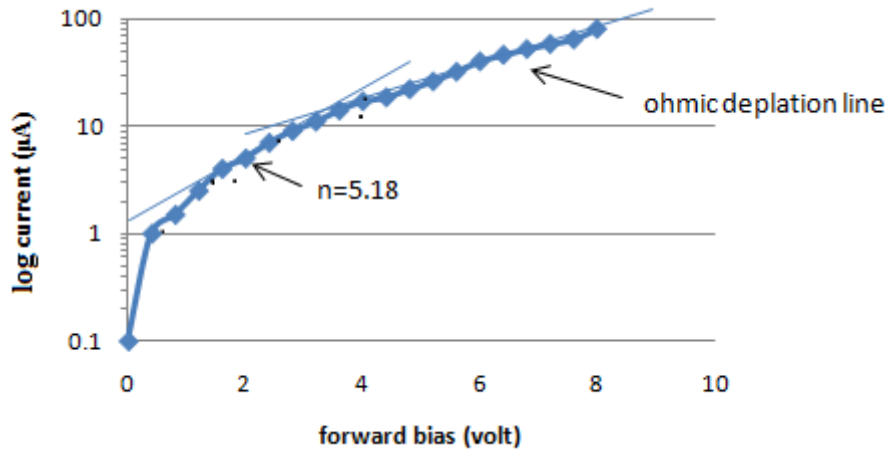


Figure.(12) The corresponding logarithmic scale in current with forward bias condition

Figure (13) shows current-voltage in reverse bias of nSnO<sub>2</sub>/SiO<sub>2</sub>/pSi hetrojunction under illumination

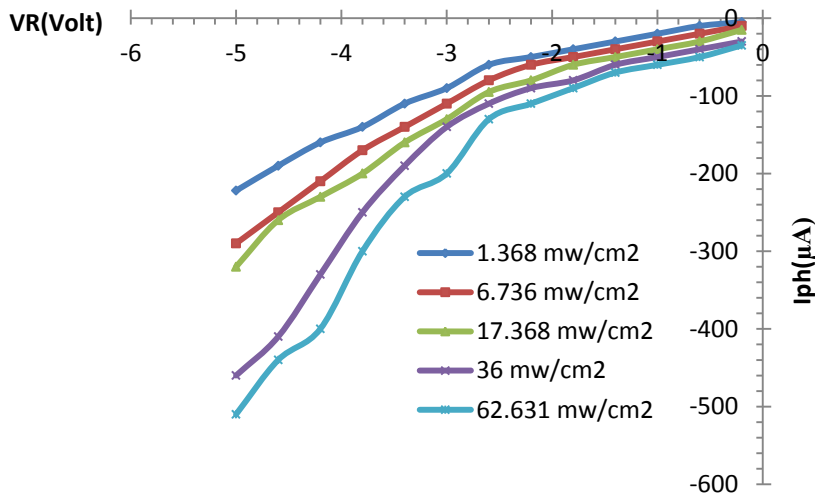


Figure.(13) current-voltage in reverse bias of nSnO<sub>2</sub>/SiO<sub>2</sub>/pSi hetrojunction under illumination with different intensity of the light

Under external reverse bias condition photocurrent caused by the nSnO<sub>2</sub>/SiO<sub>2</sub>/pSi hetrojunction exposing under illumination by white light lamp was obviously much larger than the dark current.

This result is due to the depletion region of the device extends and as a result, more incident photons will contribute to the generation of the electron-hole pairs in the depletion region. The electron-hole pairs separate from each other by internal electric field in the depletion region, which becomes large with the applied external bias.

From the above figure, we can see the photo-current increase with the increasing of incident light intensity, where the large intensity refers to a great number of incident photons and hence large of separated electron-hole pairs.

The short-circuit current ( $I_{SC}$ ) represents amount of the current that can flow through the device as a function of the incident optical power. The open-circuit voltage ( $V_{oc}$ ) represents the voltage drop across the device as a function of incident optical power.  $I_{SC}$  and  $V_{oc}$  are obtained by irradiated the detector with optical light and without connect the detector to the power supply the power of the incident light from a halogen lamp varied by variable applied voltage. Figure (14a, b) show short circuit current and open circuit voltage as a function of the incident power density for n-SnO<sub>2</sub>/SiO<sub>2</sub>/p-Si hetrojunction.

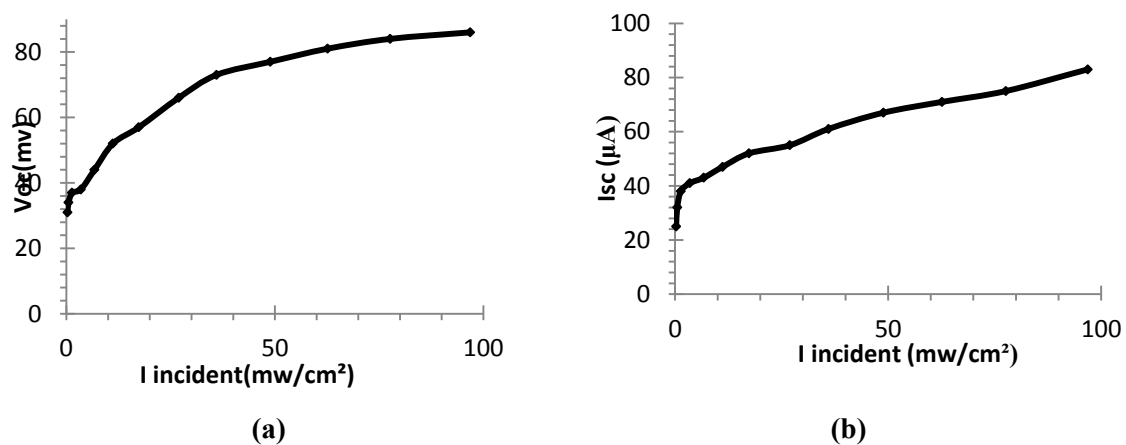


Figure (14 a, b) Short circuit current and open circuit voltage as a function of the incident power density for n-SnO<sub>2</sub>/SiO<sub>2</sub>/p-Si hetrojunction

Figure (14 a, b) shows the relation between short-circuit current ( $I_{SC}$ ) and open-circuit voltage ( $V_{OC}$ ) with the incident light intensity. From the result obtained it is observed that is a linear relation between  $I_{SC}$  and  $V_{OC}$  with the incident light intensity to reach a maximum value beyond tends to saturated and become constant. This occurs due to the total separation of the photo-generated electron-hole pairs. The linear behavior of  $V_{OC}$  versus incident power refers to good linearity of the prepared device to work as a detector or solar cell.

### CONCLUSIONS

SnO<sub>2</sub> thin film synthesis by post-thermal treatment of the deposited tin by vacuum thermal evaporation on glass and p-type silicon substrates respectively, for preparation of metal-insulator-semiconductor hetrojunction. The structural, surface morphology, optical and electrical measurements show that the SnO<sub>2</sub> thin film is high quality; it's highly absorbance in UV, where's transparent in visible and infrared regions with direct band gap is 3.6 eV, tetragonal rutile structure, nano crystalline thin film and activation energy 0.19 eV. The photovoltaic characteristics of nSnO<sub>2</sub>-SiO<sub>2</sub>-pSi-Al heterojunction have rectifying behavior, ideality factor approximately 5.18 and a linear relation between  $I_{SC}$  and  $V_{OC}$  with the incident light intensity to reach a maximum value beyond tends to saturated and become constant due to the total separation of the photo-generated electron-hole pairs.

## REFERENCE

- [1]-D. Hocine, M.S. Belkaid and K. Lagha, "Influence of interfacial oxide layer thickness on conversion efficiency of SnO<sub>2</sub>/SiO<sub>2</sub>/Si(N) Solar Cells", *Revue des Energies Renouvelables*, Vol.11 No. 3 pag. 379 – 384, (2008).
- [2]- M. S. Islam, M. F. Hossain, N. M. Shaalan and M. M. Ali, "Fabrication of Nanostructured SnO<sub>2</sub> Thin Films by A Simplified Thermal Evaporation System", *Journal of Modern Science and Technology* Vol. 1, No. 1, Issue120, pag.120-125, (2013).
- [3]- Hebo, Zhongquanma, Xujing, Zhaolei, Zhangnansheng, Lifeng, Shencheng, Shenling, Mengxiajie, Zhouchengyue, Yuzhengshan, Yinyanting", "Structural, Electrical And Optical Properties Of AZO/SiO<sub>2</sub>/P-Si SIS Heterojunction Prepared By Magnetron Sputtering, *Optica Applicata*, Vol.40, No. 1, pag.15-24, (2010).
- [4]- Areej Adnan Hateef, Marwa Abdul Muhsien Hassan, Najim A. Sumoom and Sabah Jameel, "Physical properties of SnO<sub>2</sub>: Co thin films prepared by chemical spray pyrolysis", *Journal of Zankoy Sulaimani- Part A (JZS-A)*, Vol.15, No 4, Pag 29-36, (2013).
- [5]- Asama. N. Naje, Azhar S. Norry, Abdulla. M. Suhail, "Preparation and Characterization of SnO<sub>2</sub> Nanoparticles", *International Journal of Innovative Research in Science, Engineering and Technology* Vol. 2, Issue 12, pag.7068-7072, (2013).
- [6]- H.N. Lim , R. Nurzulaikha , I. Harrison , S.S. Lim, W.T. Tan , M.C. Yeo , "Spherical Tin Oxide, SnO<sub>2</sub> Particles Fabricated Via Facile Hydrothermal Method For Detection of Mercury (II) Ions" *International Journal Of Electrochemical Science*, Vol.6, pag. 4329 – 4340, (2011).
- [7]- Khalid K. Mohammed, "The Electrical And Optical Properties Of SnO<sub>2</sub> – Si(N) Structure Solar Cells", *Al-Rafidain Engineering journal*, Vol.13 No.3, pag.1-8, (2005).
- [8]- Jun Pan, Hao Shen, and Sanjaymathur, "One-Dimensional SnO<sub>2</sub> Nanostructures: Synthesis and Applications", *Hindawi Publishing Corporation Journal of Nanotechnology*, Volume Article Id 917320, pag 1-12, (2012).
- [9]- Luqman Sufer Ali, "Preparation and Study of SnO<sub>2</sub> MOM Structure By The Thermal Vacuum Evaporation Deposition, *Al-Rafidain Engineering* Vol.22 No. 1, pag.99-111, (2014).
- [10]- Young-Il Kim, Hee-Soo Moon, Kwang-Sun Ji, Sang-Hyun Seong And Jong-Wan Park, "SnO<sub>2</sub> Thin Film Doped with Si for Negative Electrode of Microbattery in MEMS," *Journal Of The Korean Physical Society*, Vol. 39, Pag. S 337-S 340, (2001).
- [11]- M. Özer, D.E. Yıldız, Ş. Altındal, "Temperature dependence of characteristic parameters of the Au/SnO<sub>2</sub>/n-Si (MIS) Schottky diodes", *Solid-State Electronics*, Volume 51, Issue 6, , Pages 941–949, (2007).
- [12]- Agnieszka Martyła, Łukasz Majchrzycki, "Preparation of SnO<sub>2</sub> thin films for photovoltaic electrode materials using sol-gel method", *67, 12, Pag. 1207–1216*, (2013).
- [13]- Jin Ku Kwak, Kyung Hoon Park, Dong Yeol Yun, Dea Uk Lee and Tae Whan Kim "Microstructural and Optical Properties of SnO<sub>2</sub> Nanoparticles Formed by Using a Solvothermal Synthesis Method", *Journal of the Korean Physical Society*, Vol. 57, No. 6, Pag. 1803-1806, (2010).
- [14]- k s shamala, c s murthy and k narasimha rao, "studies on tin oxide films prepared by electron beam evaporation and spray pyrolysis methods", *bull. Mater. Sci.*, Vol. 27, No. 3, Pag. 295–301, (2004).
- [15]- Evan T. Salem, "Tin Oxide Nanoparticles Prepared Using Liquid Phase Laser Ablation for Optoelectronic Application" *Nanoscience and Nanotechnology*, Vol.2, No.3, Pag. 86-89, (2012).
- [16]- S.H. Luo a,b, Q. Wan a, W.L. Liu a, M. Zhang , "Photoluminescence properties of SnO<sub>2</sub> nanowhiskers grown by thermal evaporation, *Progress in Solid State Chemistry*, Vol.33, pag.287-292, (2005).

- [17]- Miguel Henrique Boratto, Luis Vicente de Andrade Scalvi, "Heterojunction between  $\text{Al}_2\text{O}_3$  and  $\text{SnO}_2$  thin films for application in transparent FET", *Material Research*, Vol.17, No. 6, pag.1420-1426, (2014).
- [18]- Aseel Mustafa Abd Al – Majed "Studying the optical and electrical properties of  $\text{Cu}_2\text{O}$  and  $\text{Bi}_2\text{O}_3$  films prepared by rapid thermal oxidation" MSc (Al-Mustansiriya University), Pag. 43, (2005).
- [19]- Geun-Hyoung Lee "Cactus-Like  $\text{SnO}_2$  Nanostructures Grown by Thermal Evaporation Technique" *Materials Transactions*, Vol. 54, No. 11, Pag. 2159 - 2161, (2013).
- [20]-P. Scherrer, *Göttinger Nachrichten Gesell.*, Vol. 2, pag. 98 ,(1918).
- [21]-e. Manea, e. Budianu, m. Purica, c. Podaru, "  $\text{SnO}_2$  thin films prepared by sol gel method for \honeycomb textured silicon solar cells" *journal of information Science and technology*, Vol. 10, No. 1, , Pag. 25-33, (2007).
- [22]-Claude Jombert, Paris, (1729).
- [23]-Adel H. Al-khayatt, Shymaa K. Hussian, " Structural and Optical characterization of Nanocrystalline  $\text{SnO}_2$  thin film prepared by spray pyrolysis technique", *Journal of Kufa – Physics*, Vol.5 No.1,Pag.69-78, (2013).
- [24]-T. Arai, "The Study of the Optical Properties of Conducting Tin Oxide Films and their Interpretation in Terms of a Tentative Band Scheme", *Journal physics Society*, Vol.15, Pag. 916-927, (1960).
- [25]- D. Patidar, K. S. Rathore, N. S. Saxena, Kananbala Sharma, T. P. Sharma , "energy band gap and conductivity measurement of cdse thin films ",*Chalcogenide Letters*, Vol. 5, No. 2, Pag 21 – 25, (2008).
- [26]- P. B. Pillai, " Extraction of Schottky barrier at the F-doped  $\text{SnO}_2/\text{TiO}_2$  interface in Dye Sensitized solar cells", *journal of renewable and sustainable energy*, Vol.6, No.013142,pag. 1-12 , (2014).